

This article was downloaded by:

On: 26 January 2011

Access details: *Access Details: Free Access*

Publisher *Taylor & Francis*

Informa Ltd Registered in England and Wales Registered Number: 1072954 Registered office: Mortimer House, 37-41 Mortimer Street, London W1T 3JH, UK



## Liquid Crystals

Publication details, including instructions for authors and subscription information:

<http://www.informaworld.com/smpp/title~content=t713926090>

### Microscopic origin of spontaneous polarization in ferroelectric $S_C^*$ liquid crystals

B. Kutnjak-urbanc<sup>a</sup>; B. Žekš<sup>b</sup>

<sup>a</sup> J. Stefan Institute, Ljubljana, Slovenia <sup>b</sup> Institute of Biophysics, Medical Faculty, Ljubljana, Slovenia

**To cite this Article** Kutnjak-urbanc, B. and Žekš, B.(1995) 'Microscopic origin of spontaneous polarization in ferroelectric  $S_C^*$  liquid crystals', *Liquid Crystals*, 18: 3, 483 – 488

**To link to this Article:** DOI: 10.1080/02678299508036648

**URL:** <http://dx.doi.org/10.1080/02678299508036648>

PLEASE SCROLL DOWN FOR ARTICLE

Full terms and conditions of use: <http://www.informaworld.com/terms-and-conditions-of-access.pdf>

This article may be used for research, teaching and private study purposes. Any substantial or systematic reproduction, re-distribution, re-selling, loan or sub-licensing, systematic supply or distribution in any form to anyone is expressly forbidden.

The publisher does not give any warranty express or implied or make any representation that the contents will be complete or accurate or up to date. The accuracy of any instructions, formulae and drug doses should be independently verified with primary sources. The publisher shall not be liable for any loss, actions, claims, proceedings, demand or costs or damages whatsoever or howsoever caused arising directly or indirectly in connection with or arising out of the use of this material.

# Microscopic origin of spontaneous polarization in ferroelectric $S_C^*$ liquid crystals

by B. KUTNJAK-URBANC\*† and B. ŽEKŠ‡

† J. Stefan Institute, Jamova 39, 61111 Ljubljana, Slovenia

‡ Institute of Biophysics, Medical Faculty, Lipičeva 2, 61105 Ljubljana, Slovenia

(Received 3 May 1994; accepted 15 July 1994)

The origin of spontaneous polarization in the ferroelectric smectic  $C^*$  phase is investigated within a mean-field microscopic model which describes the coupling between the tilt of molecules from the normal to the smectic layers and the rotation of a molecule around its long axis. The mean-field potential is studied which takes into account a chiral polar and a non-chiral quadrupolar biasing of the rotation of molecules around the molecular long axes. Each molecule is characterized by three transverse molecular axes: the chiral axis which turns parallel to the macroscopic  $C_2$  axis at small tilts, the polar axis in the direction of the transverse dipole moment and the quadrupolar axis which tends to be parallel to the  $C_2$  axis at very large tilts. A numerical analysis of the model shows that there are four different types of spontaneous polarization dependent on the temperature, including the sign-reversal type. The influence of three microscopic parameters, i.e. two angles between the three characteristic axes and the relative strength of the chiral versus the non-chiral biasing, on the type of spontaneous polarization is investigated. The relationship between the microscopic and the equivalent Landau model is established and discussed.

## 1. Introduction

The existence of ferroelectricity in chiral smectic  $C^*$  ( $S_C^*$ ) systems was first predicted by Meyer *et al.* [1]. In the ferroelectric  $S_C^*$  phase, the spontaneous polarization is a result of an ordering of molecular short axes which carry electric dipole moments. However, the average dipole moment within a smectic layer is much smaller than the dipole moment of an individual molecule [2]. Thus, the energies which give rise to the polar ordering of short axes should be comparable to the thermal energy. Thermal fluctuations of the molecular short axes, which are neglected in a phenomenological, Landau-like approach, are expected to play an essential role, especially in the limit of disappearing chirality where the Landau model gives incorrect predictions [3].

In the high-temperature smectic A ( $S_A$ ) phase the molecular director is parallel to the normal to the smectic layers. As far as the ordering of transverse molecular axes is considered, molecules feel on average an axially symmetric potential, so that there is no preferred direction of the molecular short axes, i.e. no transverse spontaneous polarization. The axial symmetry is broken at the phase transition from the  $S_A$  phase, with the local symmetry  $D_\infty$ , to the  $S_C^*$  phase, with the local symmetry  $C_2$ , where the director is tilted from the normal to the smectic layers.

In both smectic phases, the molecules possess the head-to-tail symmetry: each long axis within a layer can be oriented either up or down with equal probability, so that there is no net longitudinal polarization. In the  $S_C^*$  phase, the ordering of molecular long axes is usually described by the tilt  $\xi = (\xi_1, \xi_2)$  which is a projection of the director into a smectic plane. The tilt as the primary order parameter induces the in-plane spontaneous polarization  $\mathbf{P} = (P_x, P_y)$  which is non-zero only along the  $C_2$  axis is thus perpendicular to the tilt  $\xi$ . The spontaneous polarization is treated as a secondary order parameter. The first phenomenological description of the  $S_A \leftrightarrow S_C^*$  phase transition was given by Pikin and Indenbom [4]. In the Pikin–Indenbom model, the magnitude of the polarization  $P = |\mathbf{P}|$  within a layer is proportional to the magnitude of the tilt  $\Theta = |\xi|$ . As the tilt magnitude  $\Theta \propto \sqrt{(T_c - T)}$ , where  $T_c$  is the transition temperature, the Pikin–Indenbom model yields a spontaneous polarization which increases monotonically with lowering temperature. Due to a systematic and qualitative disagreement of the Pikin–Indenbom model with the measured thermodynamic properties [5], this model has been extended [5–8] by some additional invariants of higher order. The essential point of the extended model is the presence of a non-chiral biquadratic coupling [6] between the two order parameters, which allows also for a more general temperature dependence of the spontaneous polarization [9]. Constructing a simple microscopic model [3, 5, 10],

\* Author for correspondence.

the biquadratic coupling has been shown to originate in a quadrupolar ordering of transverse molecular axes which is usually much larger than the polar ordering, except just below the critical temperature. This microscopic model gives correct results in the limit of disappearing chirality and is equivalent to the extended Landau model [5–8] in the limit of large chiralities.

The simple microscopic model is not general enough to allow for such a complicated temperature dependence of the spontaneous polarization as the sign-reversal type which has been found in several compounds [11]. Recently, Meister and Stegemeyer [12] have introduced a microscopic model which is an extension of the simple microscopic model. This microscopic model yields an alternative explanation [12] of the sign-reversal type of polarization [11]. Moreover, recent investigations [13] of the magnitude and the sign of the spontaneous polarization as a function of the molecular structure of a series of cyclohexanone derivatives used as chiral dopants seem to support the microscopic model.

The aim of the present paper is the analysis of the microscopic model. We are interested in different types of spontaneous polarization and their dependence on the temperature. In addition we discuss the relation between the microscopic and the corresponding Landau model and derive the relationships between the parameters of the two models.

## 2. The microscopic model

In order to describe the model, three characteristic molecular axes are introduced. Molecules are treated as rigid, so that all three molecular axes are assumed to be fixed: as a molecule rotates around the long axis, all three characteristic axes rotate in such a way that the angles between the three axes remain unchanged. We associate the polar axis  $\mathbf{p}$  with the direction of the transverse electric dipole moment of a molecule. As already investigated by others [14], the transverse dipole moment is not necessarily parallel to the  $C_2$  axis. The chiral molecular axis  $\boldsymbol{\epsilon}$  is defined as a molecular short axis which orients parallel to the  $C_2$  axis at small tilts, i.e. at temperatures just below the critical temperature  $T_c$  of the  $S_A \leftrightarrow S_C^*$  phase transition. The quadrupolar axis  $\boldsymbol{\eta}$  is defined as the molecular axis which turns parallel to the  $C_2$  axis at very large tilts, i.e. at low temperatures. Meister and Stegemeyer [12] derived the microscopic model from the simple microscopic model [3, 5, 10] by omitting the assumption that the transverse chiral, polar and quadrupolar molecular axes are parallel. We denote the angle between the chiral and the polar axis by  $\beta_0$  and the angle between the chiral and the quadrupolar axis by  $\alpha_0$  as shown in figure 1. The angle  $\beta_0$  can assume any value between  $-\pi$  and  $\pi$  and  $\alpha_0$  any value between  $-\pi/2$  and  $\pi/2$  (the character of the quadrupolar ordering is such that the

angles  $\alpha_0$  and  $\alpha_0 + \pi$  are equivalent; the angle  $\alpha_0$  is chosen to be  $|\alpha_0| \leq \pi/2$  because such an orientation is energetically preferable for the chiral axis).

We define a single-particle potential  $V(\psi)$  for one molecule in the mean field of other molecules within a layer

$$V(\psi) = -a_1 \tilde{\Theta} \cos \psi - a_2 \tilde{\Theta}^2 \cos 2(\psi + \alpha_0), \quad (1)$$

where  $\psi$  is the angle between the chiral axis  $\boldsymbol{\epsilon}$  of the molecule and the  $C_2$  axis. In figure 1, the three characteristic molecular axes are presented in the  $xy$ -plane perpendicular to the director which is parallel to the  $z$  axis. Here the  $y$  axis is parallel to the  $C_2$  axis. The coefficients  $a_1$  and  $a_2$  are assumed to be positive.

The potential  $V(\psi)$  reflects breaking of the axial symmetry within a layer at the  $S_A \leftrightarrow S_C^*$  phase transition in the polar (the  $a_1$  term) and in the quadrupolar way (the  $a_2$  term). The polar term is of a chiral origin and corresponds macroscopically to the linear coupling between the tilt and the spontaneous polarization. The quadrupolar term is present in non-chiral systems as well, and yields the quadratic coupling between the two order parameters. The simple microscopic model [3, 5, 10] is a special example of the above model for  $\alpha_0 = 0$  and  $\beta_0 = 0$ .

At small tilts,  $\tilde{\Theta} \rightarrow 0$ , when the first term in the potential, given by equation (1), prevails, the most favourable orientation is  $\psi = 0$  (molecules tend to align their chiral axes along the  $C_2$  direction), whereas at large tilts,  $\tilde{\Theta} \rightarrow \infty$ , when the second term in the potential  $V(\psi)$  prevails, the most favourable orientation is  $\psi = -\alpha_0$  (molecules tend to align their quadrupolar axes along the  $C_2$  direction). This is graphically presented in figure 2, where the angles  $\alpha_0$  and  $\beta_0$  are chosen in such a way as to yield the sign-reversal type of the polarization. Due to the head-to-tail symmetry, the two orientations (up and down) are equally favourable: the other orientation is obtained by rotating the molecular axes by  $\pi$  around the  $C_2$  axis as shown in figure 2. In such a way, only the polarization along the  $C_2$  axis can be different from zero. The graphic

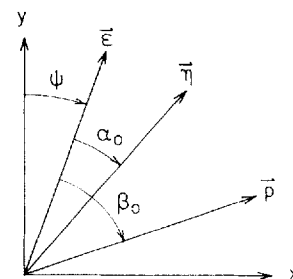


Figure 1. Definition of three characteristic transverse molecular axes for a molecule oriented up: the chiral axis  $\boldsymbol{\epsilon}$ , the quadrupolar axis  $\boldsymbol{\eta}$  and the polar axis  $\mathbf{p}$  are in the plane perpendicular to the long axis. The  $y$  axis is parallel to the  $C_2$  axis.

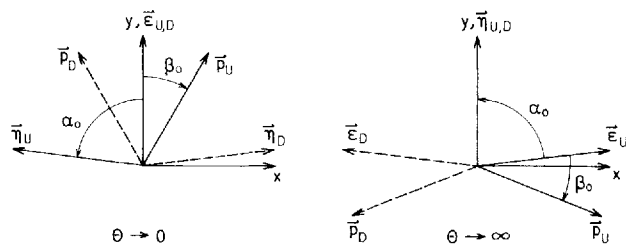


Figure 2. The orientation of the three molecular axes (a) at small tilts,  $\Theta \rightarrow 0$ , and (b) at very large tilts,  $\Theta \rightarrow \infty$ . The angles  $\alpha_0 = -\pi/3$  and  $\beta_0 = \pi/4$  are chosen in such a way as to yield the sign-reversal type of spontaneous polarization. Both orientations, for long axes oriented up (U) and down (D), are depicted.

presentation in figure 2 shows the orientation with the lowest energy. In the limit of large chirality, where thermal fluctuations can be neglected, the state with the lowest energy corresponds also to the average orientation.

The probability for a given orientation  $\psi$  to occur is proportional to the Boltzmann factor  $\exp[-V(\psi)/k_B T]$  and the averages  $\langle \cos \psi \rangle$ ,  $\langle \cos 2\psi \rangle$ , etc., are calculated by standard methods. We are interested in the spontaneous polarization  $\bar{P}$  which is proportional to the average  $\langle \cos(\psi + \beta_0) \rangle$  if one takes into account the head-to-tail symmetry (see figure 2)

$$\bar{P} = \rho p \langle \cos(\psi + \beta_0) \rangle. \quad (2)$$

Here  $\rho$  is a number density of molecules and  $p$  is an electric dipole moment of the molecule perpendicular to the long axis. The angle  $\beta_0 \neq 0$  expresses the fact that the transverse electric dipole moment of an individual molecule is in general not parallel to the  $C_2$  axis.

We introduce dimensionless quantities  $\Theta$ ,  $P$  and a dimensionless chiral parameter  $\beta$

$$\theta = \sqrt{\left(\frac{a_2}{2k_B T}\right)} \Theta, \quad P = \frac{\bar{P}}{\sqrt{2\rho p}}, \quad \beta = \frac{a_1}{2\sqrt{(k_B T a_2)}}, \quad (3)$$

so that the potential  $V(\psi)$  can be written in a dimensionless form

$$\frac{V(\psi)}{k_B T} = -2\sqrt{2}\beta\Theta \cos \psi - 2\Theta^2 \cos 2(\psi + \alpha_0). \quad (4)$$

The parameter  $\beta$  measures the importance of the chiral polar term  $a_1$  versus the non-chiral quadrupolar term  $a_2$ . The polarization  $P$  can be calculated as a function of  $\Theta^2 \propto T_c - T$  numerically. However, for small tilts  $\Theta$ , an analytic expression is found by expanding the exponent in the Boltzmann factor, whereas for very large tilts  $\Theta$  the Laplace's method [15] can be used to find the asymptotic behaviour

$$P \approx \beta\Theta \cos \beta_0, \quad \Theta \rightarrow 0, \quad (5a)$$

and

$$P \sim \cos(\beta_0 - \alpha_0)/\sqrt{2}, \quad \Theta \rightarrow \infty. \quad (5b)$$

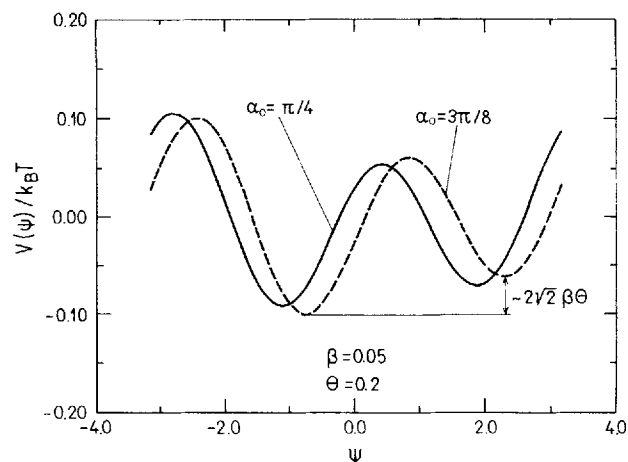


Figure 3. The mean-field potential  $V(\psi)$ , normalized to the thermal energy  $k_B T$  as a function of  $\psi$ , i.e. the orientation of the short molecular axes has two minima in the interval  $\psi \in [-\pi, \pi]$ . The energy difference between the two minima is equal to  $2\sqrt{2}|\beta|\Theta$ .

The asymptotic result given by equation (5b) is not surprising: at very large tilts  $\Theta$  the first term in the potential (4) is small compared to the second term ( $\theta^2 \gg 2\beta^2$ ), so that the most probable configuration is  $\psi = -\alpha_0$ . As presented in figure 3, the potential  $V(\psi)/(k_B T)$ , given by equation (4), has, within the interval  $\psi \in [-\pi, \pi]$ , two minima (the energy difference between the two minima divided by the thermal energy  $k_B T$  is of the order  $|\beta|\Theta$ ). If the most probable configuration at  $\Theta \rightarrow \infty$   $\psi = -\alpha_0$  is also to be the average configuration, so that  $\langle \cos(\psi + \beta_0) \rangle$  can be replaced simply by  $\cos(\beta_0 - \alpha_0)$ , one of the minima should be much more occupied than the other one, and thus  $|\beta|\Theta \gg 1$ .

### 3. Different types of the spontaneous polarization

Since the orientation with the lowest energy changes with the temperature (at small tilts, the chiral axis is parallel to the  $C_2$  axis, whereas at large tilts, the quadrupolar axis turns parallel to the  $C_2$  axis), the average molecular orientation also rotates around the long axis as the temperature changes. Thus, various types of spontaneous polarization dependent on the temperature are expected for different values of the two characteristic molecular angles.

At a fixed chiral parameter  $\beta$ , different types of the spontaneous polarization  $P$  dependent on the square of the tilt  $\Theta^2 \propto T_c - T$  can be classified into four groups. In figure 4, the four different types of the spontaneous polarization  $P$  obtained numerically are depicted: the sign-reversal type ( $P$  changes its sign), the monotonic type ( $P$  grows monotonically with  $\Theta^2 \propto T_c - T$ , its second derivative  $d^2 P/d(\Theta^2)^2$  is negative), the S-shaped type ( $P$  is

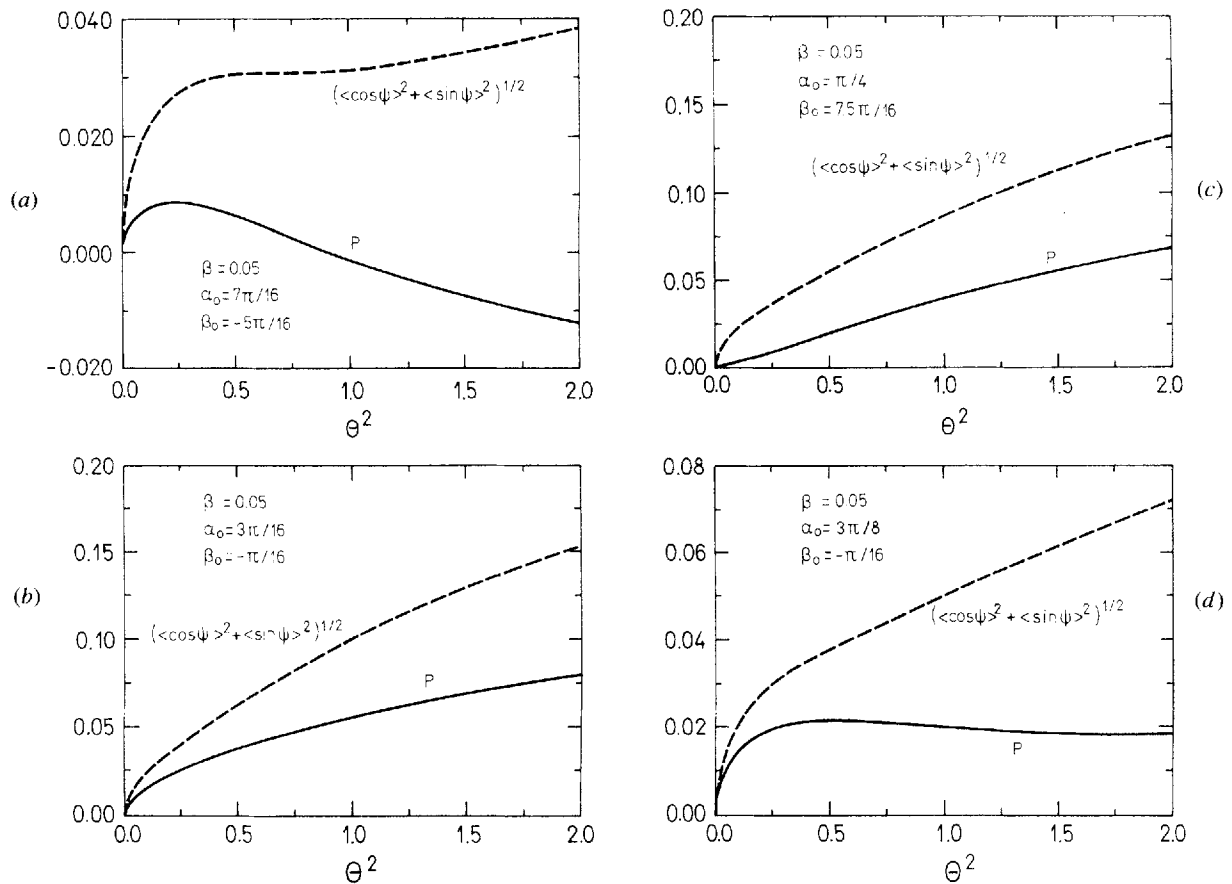


Figure 4. The four different types of spontaneous polarization are presented by full lines: (a) the sign-reversal type, (b) the monotonic type, (c) the S-shaped type and (d) the non-monotonic type. The dotted curves correspond to the polar ordering which increases monotonically on lowering the temperature.

a monotonic function of  $\Theta^2$ , but the second derivative  $d^2P/d(\Theta^2)^2$  changes its sign) and the non-monotonic type ( $P$  is positive, but a non-monotonic function of  $\Theta^2$ ). Although the polarization itself is not necessarily a monotonic function of the temperature, the polar ordering which is proportional to  $\sqrt{\langle \cos \psi \rangle^2 + \langle \sin \psi \rangle^2}$  increases monotonically with decreasing temperature as is also shown in figure 4.

We consider only such angles  $\alpha_0$  and  $\beta_0$  which yield a positive polarization in the limit  $\Theta \rightarrow 0$ , i.e. the angle  $\beta_0$  assumes the values between  $-\pi/2$  and  $\pi/2$ . Further we restrict ourselves to  $\alpha_0 \in [0, \pi/2]$ . One can cover the area  $\alpha_0 \in [-\pi/2, 0]$  by taking into account the head-to-tail symmetry: the system is invariant under the transformation  $\alpha_0 \rightarrow -\alpha_0$  and  $\beta_0 \rightarrow -\beta_0$  (inversion in the plane).

The areas of different types in the parameter space  $(\alpha_0, \beta_0)$  are presented in figure 5, where the chiral parameter  $\beta$  increases from  $\beta = 0.01$  to 5. The boundaries between the areas of different types have been determined numerically: on a discrete lattice ( $20 \times 40$ ) of the

parameter space  $(\alpha_0, \beta_0)$ , the type of spontaneous polarization  $P$  has been determined by checking the reversal of the sign of  $P(x)$  or  $dP(x)/dx$  or  $d^2P(x)/dx^2$ . Here  $x = \Theta^2 \in [0, \Theta_{\max}^2]$ , where at each value of the chiral parameter  $\beta$  the value  $\Theta_{\max}$  has been chosen to be large enough to reach the asymptotic regime where the expression (5 b) is valid. The area of the sign-reversal type of polarization is independent of the chiral parameter  $\beta$  and assumes  $\frac{1}{4}$ th of the total area. The sign-reversal type of polarization occurs at such combinations of the two angles which yield negative asymptotic values of the polarization, i.e.  $\cos(\beta_0 - \alpha_0) < 0$  (see figure 2). The area of the S-shaped polarization is larger at smaller values of the chiral parameter  $\beta$  and goes to zero at large values of  $\beta$ , whereas the area of the non-monotonic type of spontaneous polarization increases with  $\beta$ . In the limit of a very large chiral parameter  $\beta$ , the non-monotonic type occurs at  $\alpha_0 \in (\beta_0, \beta_0 + \pi/2)$  which can also be understood by considering the construction related to the orientation with the lowest energy in figure 2.

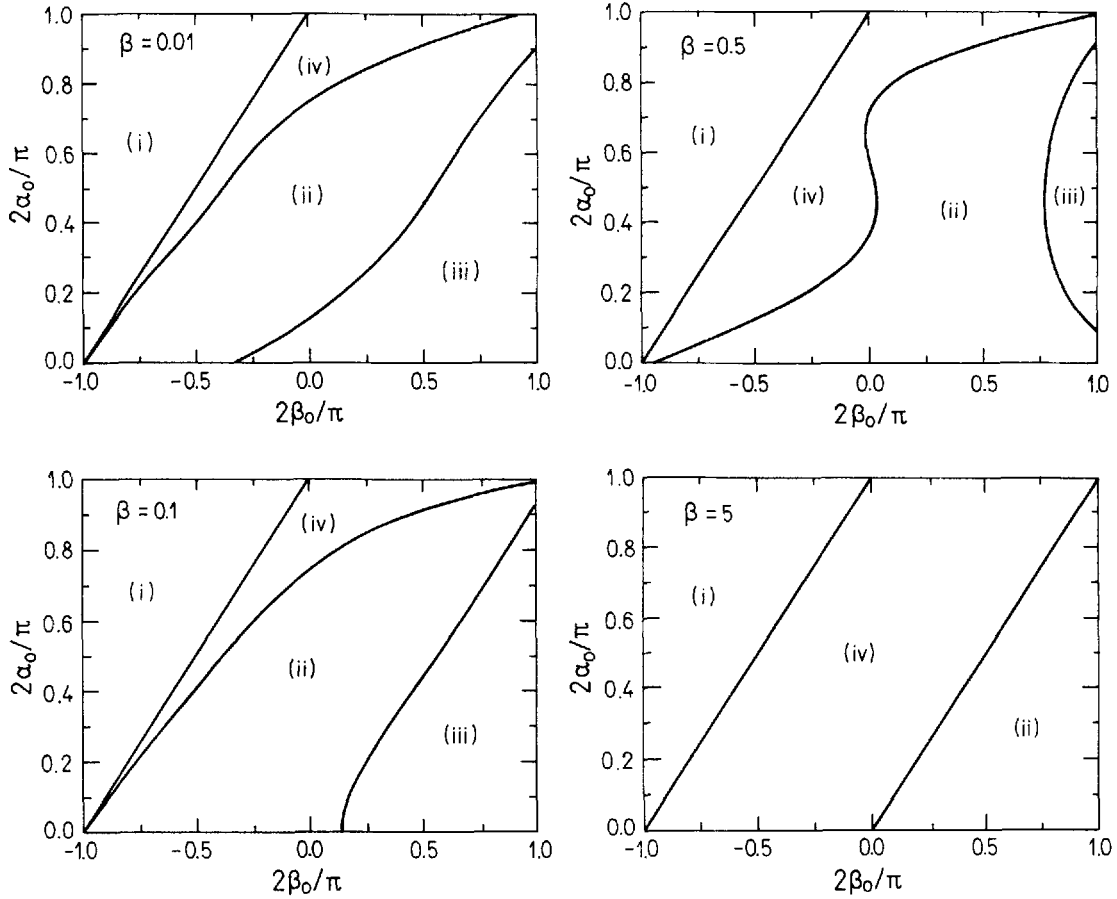


Figure 5. Diagrams show the areas of the four different types of spontaneous polarization in the parameter space of the two angles ( $\alpha_0, \beta_0$ ). The four different diagrams are associated with the following values of the chiral parameter,  $\beta = 0.01, 0.10, 0.50, 5.0$ . The area of the sign-reversal type is denoted by (i), (ii) corresponds to the monotonic type, (iii) to the S-shaped type and (iv) to the non-monotonic type.

#### 4. Relationship between the microscopic and the Landau model

Here we want to compare the microscopic model to the phenomenological Landau model. We are interested in a relationship between the parameters of the two models. Especially, we would like to show how to describe the sign-reversal type of the spontaneous polarization within the Landau model.

In the Landau model the part of the free energy density which depends on the polarization  $\mathbf{P} = (\tilde{P}_x, \tilde{P}_y)$  reads

$$f_{\mathbf{P}} = \frac{1}{2\epsilon} (\tilde{P}_x^2 + \tilde{P}_y^2) + \frac{\eta}{4} (\tilde{P}_x^2 + \tilde{P}_y^2)^2 + C(\tilde{P}_x \xi_2 - \tilde{P}_y \xi_1) - \frac{\Omega}{2} (\tilde{P}_x \xi_2 - \tilde{P}_y \xi_1)^2, \quad (6)$$

where the tilt  $\xi$  is the primary and the polarization  $\mathbf{P}$  the secondary order parameter of the  $S_A \leftrightarrow S_C^*$  phase transition. For simplicity we omit the flexoelectric term in the expression given by equation (6).

The free energy density expression can be calculated on the basis of the microscopic model via the statistical sum over all possible molecular orientations  $\psi$  by taking into account the mean-field potential  $V(\psi)$ , given by equation (1). It can be shown that the coefficients in the free energy density expansion in equation (6) are related to the coefficients  $a_1$  and  $a_2$  of the microscopic model

$$C = \lambda \frac{a_1}{p}, \quad \Omega = \lambda^2 \cos 2\alpha_0 \frac{a_2}{qp^2}, \\ \epsilon = \lambda^{-2} \frac{qp^2}{2k_B T}, \quad \eta = \lambda^4 \frac{k_B T}{q^3 p^4}, \quad (7)$$

where  $\lambda$  is given by

$$\lambda^{-1} = \cos \beta_0. \quad (8)$$

The relationships, given by equation (7) and (8), are obtained by taking into account the lowest order terms in the free energy density expansion. Within the simple microscopic model, the relationship between the

microscopic and the macroscopic parameters is established by putting  $\lambda = 1$  and  $\alpha_0 = 0$  into equations (7).

After deriving the relationships, given by equations (7) and (8), we would like to find out how to account for different types of spontaneous polarization within the Landau model. It turns out that in order to describe also the sign-reversal type of the spontaneous polarization, another piezoelectric coefficient  $\kappa$  of a higher order has to be added to the free energy density expansion, given by equation (6), in addition to the piezoelectric coefficient  $C$  as has been predicted already [9]. The corresponding term which should have an opposite sign to the sign of the piezoelectric term has to be of an invariant form

$$+ \kappa(\xi_1^2 + \xi_2^2)(\bar{P}_x \xi_2 - \bar{P}_y \xi_1), \quad (9)$$

so that the polarization would change its sign at the temperature where  $C + \kappa \bar{\Theta}^2 = 0$ . Microscopically, the constants  $C$  and  $\kappa$  are related to  $a_1$ ,  $a_2$ ,  $\alpha_0$  and  $\beta_0$  through the relationships

$$C = \frac{a_1}{(\cos \beta_0)p}, \quad \kappa = -\frac{a_1 a_2}{2pk_B T} \frac{\sin \beta_0 \sin 2\alpha_0}{\cos^2 \beta_0}. \quad (10)$$

The two macroscopic coefficients  $\varepsilon$  and  $\eta$  are according to the relationships in equations (7) and (8) of an entropic origin. The expression for  $\varepsilon$  in equations (7) equals the Curie free dipole susceptibility with the renormalized electric dipole moment  $p \cos \beta_0$ .

## 5. Discussion

To summarize, we have studied the microscopic model with three characteristic molecular axes which accounts for several different types of spontaneous polarization which, are dependent on the temperature, depending on the values of the two angles between the three molecular axes. The relationship between the microscopic and phenomenological parameters has been established, showing that in order to account also for the sign-reversal type of spontaneous polarization, a piezoelectric invariant of higher order should be added to the Landau free energy expansion.

According to the microscopic model there are, in addition to the tilt which is the primary order parameter of the  $S_A \leftrightarrow S_C^*$  phase transition, another two order parameters which are induced by the tilt and are thus secondary order parameters. Both are related to the partial ordering of molecular short axes. The polarization which is a result of the polar biasing of the rotation around molecular long axes is present in chiral systems only, whereas the quadrupolar order parameter which is a consequence of a

bipolar ordering of molecular short axes exists in the non-chiral  $S_C$  phase as well. Regarding the relaxation modes related to fluctuations of the three order parameters around the equilibrium, three relaxation modes are expected to exist in the  $S_A$  phase: one is the in-phase excitation mode (the soft mode), and the other two are related to the out-of-phase relaxation of the polarization and the tilt (the polarization mode) and the quadrupolar order parameter and the tilt (the quadrupolar mode), respectively. The quadrupolar mode could not be detected in a dielectric experiment due to its non-polar character, but it could be in principle detected optically. One of the predictions of the microscopic models is therefore the existence of the quadrupolar order parameter which is expected to affect the fluctuation spectrum of the chiral and non-chiral  $S_A$  and  $S_C^*$  ( $S_C$ ) phases.

Support from the Ministry of Science and Technology of the Republic of Slovenia is acknowledged.

## References

- [1] MEYER, R. B., LIÉBERT, L., STRZELECKI, L., and KELLER, P., 1975, *J. Phys. Lett., Paris*, **36**, L69.
- [2] SELIGER, J., ŽAGAR, V., and BLINC, R., 1978, *Phys. Rev. A*, **17**, 1149.
- [3] ŽEKŠ, B., and URBANC, B., 1991, *Ferroelectrics*, **113**, 151.
- [4] PIKIN, S. A., and INDENBOM, V. L., 1978, *Usp. Fiz. Nauk*, **125**, 251; 1987, *Soviet Phys. Usp.*, **21**, 487.
- [5] ŽEKŠ, B., CARLSSON, T., FILIPIČ, C., and URBANC, B., 1988, *Ferroelectrics*, **84**, 3.
- [6] ŽEKŠ, B., 1984, *Molec. Crystals liq. Crystals*, **114**, 259.
- [7] DUMRONGRATTANA, S., and HUANG, C. C., 1986, *Phys. Rev. Lett.*, **56**, 5.
- [8] CARLSSON, T., ŽEKŠ, B., FILIPIČ, C., LEVSTIK, A., and BLINC, R., 1988, *Molec. Crystals liq. Crystals*, **163**, 11.
- [9] CARLSSON, T., ŽEKŠ, B., FILIPIČ, C., and LEVSTIK, A., 1984, *Molec. Crystals liq. Crystals*, **114**, 259.
- [10] URBANC, B., and ŽEKŠ, B., 1989, *Liq. Crystals*, **5**, 1075.
- [11] PATEL, J. S., and GOODBY, J. W., 1987, *Phil. Mag. Lett.*, **55**, 283. PATEL, J. S., and GOODBY, J. W., 1987, *Molec. Crystals liq. Crystals*, **114**, 117. GLASS, A. M., GOODBY, J. W., OLSON, D. H., and PATEL, J. S., 1988, *Phys. Rev. A*, **38**, 1673.
- [12] MEISTER, R., and STEGEMEYER, H., 1993, *Ber. Bunsenges. chem. Phys.*, **97**, 1242.
- [13] OSIPOV, M. A., MEISTER, R., and STEGEMEYER, R., 1994, *Liq. Crystals*, **16**, 173.
- [14] STEGEMEYER, H., MEISTER, R., ELLERMANN, K. H., ALTENBACH, H. J., and SUCROW, W., 1992, *Liq. Crystals*, **11**, 667. STEGEMEYER, H., MEISTER, R., ALTENBACH, H. J., and SZEWZYK, D., 1993, *Liq. Crystals*, **14**, 1007.
- [15] ERDELYI, A., 1956, *Asymptotic Expansions* (Dover Publications, Inc.). FEDORYUK, M. V., 1977, *Metod perevala* (Nauka).